



HAL
open science

Stratigraphic simulations of the shelf of the Gulf of Lions: Testing subsidence rates and sea-level curves during the Pliocene and Quaternary

Estelle Leroux, Marina Rabineau, Daniel Aslanian, Didier Granjeon, Laurence Droz, Christian Gorini

► To cite this version:

Estelle Leroux, Marina Rabineau, Daniel Aslanian, Didier Granjeon, Laurence Droz, et al.. Stratigraphic simulations of the shelf of the Gulf of Lions: Testing subsidence rates and sea-level curves during the Pliocene and Quaternary. *Terra Nova*, 2014, 26 (3), pp.230-238. <10.1111/ter.12091>. <insu-00948717>

HAL Id: insu-00948717

<https://insu.hal.science/insu-00948717v1>

Submitted on 24 Feb 2014

HAL is a multi-disciplinary open access archive for the deposit and dissemination of scientific research documents, whether they are published or not. The documents may come from teaching and research institutions in France or abroad, or from public or private research centers.

L'archive ouverte pluridisciplinaire **HAL**, est destinée au dépôt et à la diffusion de documents scientifiques de niveau recherche, publiés ou non, émanant des établissements d'enseignement et de recherche français ou étrangers, des laboratoires publics ou privés.



HAL Authorization

33

34 1. INTRODUCTION

35 1.1. GEOLOGICAL SETTING

36 The Gulf of Lions (Fig. 1) is an Upper Eocene passive margin, which results from the westward rotation of the Corsica-
37 Sardinia block and the simultaneous opening of a micro-ocean, the Liguro-Provençal basin (Montigny et al., 1981; LeDouaran
38 et al., 1984; Réhault et al., 1984; Malinverno & Ryan, 1986; Olivet, 1987; Genesseeux et al., 1989; Gorini et. al, 1993;
39 Mauffret et al., 1995; Olivet, 1996). This Western Mediterranean basin is a natural laboratory for climatic and stratigraphic
40 researches because of its connection with the Atlantic Ocean (through the Gibraltar Strait), its huge sedimentation and
41 subsidence rates and its exceptionnal data set. Moreover its sedimentological record shows a very clear paleobathymetric and
42 chronostratigraphic marker: the Messinian Margin Erosional Surface (MES) very well observed on the Liguro-Provençal
43 margin (Savoye and Piper, 1991; Gorini et al., 1994; Guennoc et al., 2000; Lofi et al., 2005; Bache et al., 2009; Lofi et al.,
44 2011). The closure of the Gibraltar Strait (Hodell et al., 1989; Krijgsman et al., 1999), associated with a strong evaporation rate
45 (enhanced by a climate change) led to a drastic Mediterranean sea-level fall at the end of the Miocene (Barr and Walker, 1973;
46 Chumakov, 1973; Clauzon, 1973; Hsü et al., 1973; Ryan, 1973), together with an intensive erosion of the margin. The MES,
47 witness of this famous Messinian salinity crisis, has then been fossilized during the Zanclean transgression and high stand of
48 sea-level. This MES surface constitutes the lowest marker of our study, in which we will try to quantify and/or point out
49 factors affecting Plio-Quaternary sedimentation.

50

51 1.2. DATA and EARLIER INTERPRETATION

52

53 This work is based on the industrial seismic survey (LRM) realized in 1996 by Total and correlations with boreholes data. No
54 detailed stratigraphic analyses have been performed on the Pliocene-Quaternary so that chronostratigraphic markers in this
55 interval must be defined (Fig. 2).

56

57 The overall geometry of Pliocene-Quaternary strata shows prograding clinoforms (or prisms) with a clear geometrical change
58 of the Late Pliocene to Quaternary clinoforms (after horizon p11, Fig. 2), from essentially prograding to prograding-aggrading.
59 In more details, the comparison between earlier studies on Pliocene to Quaternary sedimentary record in the area shows
60 similarities but also conflicting seismic interpretations (Fig. 3). Whilst the Zanclean/Piacenzian transition around 3.6–3.8 Ma is
61 indeed picked out in the same way and at the same position by Rabineau et al. (2001), Lofi (2003) and Duvail et al. (2005)
62 (blue p7 and red p6 horizons on the Fig. 3), these authors diverge about the stratigraphic position of the Pliocene/Pleistocene
63 transition (2.6 Ma) (blue p11 and red p7 horizons on the Fig. 3). The exact position of the change between Pliocene prograding
64 geometry and Pleistocene progradation-aggradation also varies with authors: the flat boundary horizon is identical in Rabineau

65 (2001) and Duvail et al. (2005), but the sloping part of the horizon is much steeper in Duvail et al. (2005). On the other hand,
66 according to the small amount of sediments, which would be accumulated after 3.8 Ma compared to that deposited in the lower
67 Pliocene, Lofi (2003) suggests attributing an age younger than 2.7 Ma to a reflector slightly above blue horizon p11.
68 But the most significant difference is about the origin of the change from prograding to prograding-aggrading geometry, which
69 has been explained by different scenarii concerning the Plio-Quaternary subsidence on the shelf. By measuring the topset
70 slopes of the Plio-Quaternary prisms and the accomodation, Rabineau (2001) estimate a constant subsidence rate since 5.32
71 Ma (a seaward tilt of the margin reaching 255 m/My at 70 km of the coast, with a rotation point at 13 km upstream the present
72 day coastline), whereas the spatial organization of offlap-break led Duvail et al. (2005) to consider an increasing subsidence
73 rate after his p6 marker (red in the Fig. 3) estimated at 2.6 Ma. Lofi et al. (2003) dit not estimate the subsidence.

74
75 The purpose of this study is to test this constant and some varying subsidence rates and constrain the above hypotheses by
76 using numerical stratigraphic modelling.

77 2. METHODS

78 Sequence stratigraphic conceptual models (e.g. Catuneanu et al, 2009) are very helpful to analyze the sedimentary record, and
79 decipher the relative role of key parameters such as accommodation and sediment supply. Stratigraphic forward numerical
80 models have been developed since the early 1960s to test these conceptual frameworks and help understanding the role of each
81 parameter on the overall stratigraphic architecture. Models intend to reproduce the dynamics of sedimentary systems.

82
83 Dionisos is a process-based modelling tool developed at IFP-Energies Nouvelles (Granjeon, 1997; Granjeon and Joseph,
84 1999) which successfully reproduced 2D and 3D overall geometry and lithology of a variety of siliciclastic case studies in
85 coastal plain, littoral, deltaic, shoreface and offshore environments (Rabineau, 2001; Rabineau et al., 2005; Jouet, 2007; Csato
86 et al., 2012) but also on the slope and the deep-sea environments (Euzen et al., 2004) and in carbonate environments (Burgess
87 et al., 2006); it has also been used to test the impact of icehouse *versus* greenhouse related sea-level curves (Sømme et al.,
88 2009).

89
90 Our purpose is to reproduce the last 5 Ma geometry of strata and the position (in distance and depth) of the chronohorizons
91 observed along the seismic profile LRM18 (Figs. 1, 2) in different subsidence scenarii:

92 1) we first measure on the profile the horizontal position of the offlap-breaks of the major prisms. They are called p4, p7, p11,
93 q10 and seafloor according to Rabineau (2001) (blue dots in the Fig. 3) and p3, p4, p5, p6, p7 according to Duvail et al. (2005)
94 (red dots in the Fig. 3)

95 2) we create fictive wells in each of these positions (Fig. 4A)

96 3) we calculate by iteration the sedimentary fluxes that give the best adjustment between the simulated and real (interpreted)
97 offlap-breaks (Fig. 4)

98

99 In a second time, we tested the impact of two eustatic curves on respectively third- and fifth-order scales on the shelf
100 morphology.

101 Details of Dionisos and input parameters quantification used in this study are described in supporting information.

102 3. SIMULATION RESULTS

103

104 3.1. SUBSIDENCE

105

106 The simulation using a constant rate of subsidence (250 m/My) enables a good reproduction of prograding then prograding-
107 aggrading geometries (Fig. 4A). These geometrie are so linked to the fluxes and to the sea-level variations during the
108 rebuilding of the shelf, after the Messinian Crisis. The simulations using non-constant subsidence rate fail to reproduce the
109 clinofoms heights if the Pliocene subsidence is null or too small (Fig. 4B2-B3). The Pleistocene subsidence is then too strong
110 and the height of final Pliocene clinofoms (which suffer the Pleistocene subsidence) is too small (even with higher Pliocene
111 sediment fluxes). It means that a strong increase in subsidence (for the Quaternary) cannot restitute the clinofoms geometries.
112 The only good restitution of the sedimentary record (Fig. 4-B1) is reached with the Pliocene (5.32 Ma-2.6 Ma) subsidence rate
113 higher than 200 m/My, followed by a subsidence rate lower than 300 m/My. The maximal subsidence acceleration to allow a
114 good reproduction of the geometry is therefore lower than 100 m/My (50%).

115 On the other hand, smaller scale subsidence rates have also been tested independently using Upper Quaternary erosional
116 surfaces over the last 450 000 years and showed an average rate of subsidence on the outer shelf of 240 m/My (Rabineau et al.,
117 2005, 2006, 2007). This value has been confirmed by the ground-truth datation of sequences using the Promess-1 drilling site
118 PRGL2 (Bassetti et al., 2008) and PRGL1 (Sierro et al., 2009).

119

120 3.2. EUSTATISM

121

122 The resolution of the sea-level curve used to run the stratigraphic model is an essential parameter for the modeling of the
123 detailed spatial repartition of deposits, lithologies and erosional areas. Fig. 5 shows how the frequency and amplitude of
124 eustatic cycles strongly influence the geometries of simulated deposits. In both cases, subsidence rate and sedimentary flux
125 remain constant.

126 The first case (A) represents a simulation using the (Haq et al., 1987) sea-level curve. The offlap-break trajectory line appears
127 segmented, with alternance of oceanwards and landwards movements (progradation/rétrogradation) following the five major

128 eustatic cycles of the Haq's curve. At our time-scale, a third order eustatic curve, like Haq's curve, emphasizes large scale
129 amplitudes of sea-level falls and rises, and favors erosion of prior transgressive system tracks during major regression. The
130 simulation does not reproduce observed geometries (compare Figs. 5A and 2).

131 The second case (B), represents a simulation using a higher resolution sea-level curve resulting from $\delta^{18}\text{O}$ data (Liesiecki and
132 Raymo, 2005). The offlap-break trajectory appears more continuous with smaller shifts of the offlap-break due to weaker
133 amplitudes of eustatic variations and a clearer prograding to a prograding-aggrading dynamic transition in good correlation
134 with observed geometries (compare with Fig. 2). The high frequencies of $\delta^{18}\text{O}$ data led to individualize more regressive/
135 transgressive cycles (and erosional surfaces) similar to those highlighted in the Quaternary (Aloisi, 1986; Rabineau, 2001;
136 Rabineau et al., 2005; Jouet, 2007) and confirmed by the recent Promess borehole (Bassetti et al., 2008).

137

138

139 3.3. SEDIMENT FLUX AND WATER DISCHARGE

140 The fluvial water discharge may be assumed as a function of climate (through precipitation and evaporation) and the size of the
141 drainage area. The drainage area does not change in the simulation, the water discharge will then reflect primarily the climate
142 (the main humidity trends).

143 Fig. 6 presents the sediment fluxes and water discharge given by simulations using the two tested sea-level curves. In both
144 cases, Early Pliocene fluxes are relatively small (18-25 km³/My), whereas Late Pliocene and Quaternary fluxes are higher (95-
145 100 km³/My), which implies a considerable increase of sediment supply around 3.8 Ma. The water discharge evolves in the
146 same way: after 3.8 Ma, a three fold increase is observed (from 100 to 300 m³/s).

147

148 4. DISCUSSION

149 The evolution of water discharge is consistent with climate simulations for the Piacenzian interval of the late Pliocene
150 indicating high precipitation in northwestern Europe (Jost et al., 2009).

151 Increase of sediment fluxes may be connected with the first cooling event at Zanclean / Piacenzian transition. The $\delta^{18}\text{O}$ record
152 on the last 5 Ma indicates a step by step climatic deterioration which testifies the transition from a Messinian warm climate to a
153 colder Pleistocene one (Shackleton et al., 1995; Lisiecki & Raymo, 2005). Major cooling events existed since the Lower
154 Pliocene, as attested by isotopic and palynologic signals (Suc et al., 1995; Popescu et al., 2010): Lower Pliocene is
155 characterized by short-term and low amplitude temperature fluctuations. The first cooling event recorded around 3.5 Ma
156 corresponds to a global climate change due to the extension of continental ices in the Northern Hemisphere (Lear et al., 2000;
157 Zachos et al., 2001). This event is also associated with extinction of planktonic foraminiferas (Rio et al., 1990) and the major
158 sea-level fall named TB 3.4-3.5 cycle by Haq et al. (1987). This cooling episode may imply an increase of the terrigenous
159 sedimentation in our basin by amplifying erosion on land. The increased and/or more efficient glacial erosion would bring

160 more detrital material to rivers and basin. We can also suppose that drift ices trap important quantities of detrital particles,
161 which are then discharged in the ocean (during the melt periods).

162 As Clauzon (1987) shown, the main part of Early Pliocene detrital sediments was trapped upstream from the shelf for the
163 filling of the onshore Messinian incisions and the Gilbert-deltas construction. We infer that the Gilbert deltas have been first
164 completely filled onshore, then allowing downstream delivery of sediments and the increase of the sediments fluxes in the
165 shelf offshore. This is consistent with the well-known marine-continental transition and the Pliocene abandonment surface
166 preceding the earliest glacial at 2.6 Ma observed on present-day onshore outcrops (Clauzon et al., 1995; Clauzon, 1996).

167 A second cooling event happened around 2.6 Ma. It follows the emergence of glacial/interglacial cycles in northern
168 Hemisphere since 3.0 Ma-3.2 Ma (Shackleton et al., 1995; Zachos et al., 2001) with an increase of floating ices in North
169 Atlantic (Backman, 1979). Faster climatic variations and higher frequency relative sea-level fluctuations occurred after that
170 period. A worldwide transition, called the "Mid Pleistocene Revolution", took place at Early to Mid Pleistocene. That
171 transition reflects a fundamental change in terrestrial climatic cyclicity: the yet overwhelming obliquity (41 ka cycles) is
172 progressively supplanted by greater amplitudes cycles (100 ka cycles). This change is dated around 0.8-0.9 Ma, and came
173 along a worldwide ice-volume growth (Head and Gibbard, 2005). Contrarily to the first major cooling at 3.8 Ma, these last
174 climatic events do not modify the detrital budget in our study area. However we must highlight that our simulations were
175 restricted to the shelf and we suggest that an important part of the sediments has been discharged to the slope and the deep
176 basin after 3.8 Ma and more specifically after 1 Ma. Further modellings integrating the deep basin are necessary to generalize
177 these partial observations and establish consistent source-to-sink sedimentary budgets.

178 5. CONCLUSIONS

179 Stratigraphic simulations enabled us to test different hypotheses on subsidence rates and sea-level variations.

180 First, the simulation using a subsidence taking the form of a tilt but with a constant subsidence rate trough time (250 m/My at
181 70 km from the coast for the entire Pliocene-Quaternary) offers a good restitution of clinoform geometries with a change from
182 an Early Pliocene essentially prograding to a Pleistocene prograding-aggrading pattern. Simulated geometries obtained with a
183 variable rate of subsidence are realistic only if the acceleration of subsidence after 2.6 Ma is reduced (from 200 m/My to 300
184 m/My). Simulation with important increase in subsidence rate through time could not fit the observed geometries and the
185 constant (or almost constant) subsidence is therefore confirmed by our study.

186 Furthermore, the simulation with a high resolution sea-level curve led to more detailed clinoform restitution than a third order
187 sea-level curve (Haq et al., 1987).

188 Finally, simulations showed an increase of sediment supply around 3.8 Ma on the shelf. It might be related to the beginning of
189 a global climate cooling in the Northern Hemisphere or to the end of the upstream trapping of the sediments into the *Gilbert*
190 *Deltas* in relation with the Messinian Salinity Crisis.

191

192

193

194 **Acknowledgements:**

195 Stratigraphic simulations were performed with IFP-Energies Nouvelles Dionisos software kindly made available to the
196 University of Brest. We would like to thanks Audrey Gailler which has helped us to use the velocity model. This research was
197 mainly funded by CNRS and IFREMER, with additional support from the French Actions-Marges and CNRS-INSU SYSTER
198 program (EROGOL). This work also benefited from the Labex Mer initiative, a State Grant from the French Agence Nationale
199 de la Recherche (ANR) in the Program « Investissements d'avenir » with the reference ANR-10-LABX-19-01, Labex Mer.

200

201 **REFERENCES:**

202

203 Aloïsi, J.C., 1986. Sur un modèle de sédimentation deltaïque: contribution à la connaissance des marges passives. PhD thesis,
204 University of Perpignan, 162 p.

205

206 Backman, J., 1979. Pliocene biostratigraphy of DSDP Sites 111 and 116 from the North Atlantic Ocean and the age of the
207 Northern Hemisphere Glaciation. *Stockl. Contr. Geol.*, **32**, 115-137.

208

209 Barr, F., and Walker, B., 1973. Late Tertiary channel system in northern Libya and its implications on Mediterranean sea level
210 changes. In: *Initial Reports of Deep Sea Drilling Project*, W.B.F. Ryan and K.J. Hsü (Eds.), U.S. Government Printing Office,
211 Washington, D.C., **13**, Part 2, 1244–1250.

212

213 Burgess, P.M., Lammers, H., van Oosterhout, C. and Granjeon, D., 2006. Multivariate sequence stratigraphy: Tackling
214 complexity and uncertainty with stratigraphic forward modeling, multiple scenarios, and conditional frequency maps. *Am.*
215 *Assoc. of Petr. Geol. Bulletin*, **90**, 1883-1901.

216

217 Catuneanu, O, Abreu, V., Bhattacharya, J.P., Blum, M.D., Dalrymple, R.W., Eriksson, P.G., Fielding, C.R., Fisher, W.L.,
218 Galloway, W.E., Gibling, M.R., Giles, K.A., Holbrook, J.M., Jordan, R., Kendall, C.G.St.C., Macurda, B., Martinsen, O.J.,
219 Miall, A.D., Neal, J.E, Nummedal, D., Pomar, L., Posamentier, H.W., Pratt, B.R., Sarg, J.F., Shanley, K.W., Steel, R.J.,
220 Strasser, A., Tucker, M.E. and Winker, C., 2009. Towards the standardization of sequence stratigraphy. *Earth-Sci. Rev.*, **92** (1-
221 2), 1-33.

222

223 Chumakov, I., 1973. Pliocene and pleistocene deposits of the Nile valley in Nubia and Upper Egypt., In: *Initial Report of Deep*
224 *Sea Drilling Project*, W.B.F. Ryan, K.J. Hsü and al.(Eds), U.S. Government Printing Office, Washington, D.C., **13**, 1242–

225 1243.

226

227 Clauzon, G., 1973. The eustatic hypothesis and the pre-pliocene cutting of the rhône valley. In: *Initial Report of the Deep Sea*
228 *Drilling Project*, W.B.F. Ryan, K.J. Hsü (Eds.), U.S. Government Printing Office, Washington, D.C., **13**, 1251–1256.

229

230 Clauzon, G., 1987. Neogene geodynamical evolution of a pyreneo-mediterranean graben: the roussillon example (southern
231 france). In: *Proceedings of the VIIIth Congress of the Regional Committee on Mediterranean Neogene Stratigraphy* (D.
232 Margit, eds) Symposium on European late Cenozoic mineral resources, Annals of the Hungarian Geological Institute,
233 Budapest, **70**, 220–226.

234

235 Clauzon, G., 1996. Limites de séquences et évolution géodynamique. *Géomorphologie*, **1**, 3–22.

236

237 Clauzon, G., Rubino, J.-L., Suc, J.-P., 1996. Les rias pliocènes du Var et de Ligurie: comblement sédimentaire et évolution
238 géodynamique. Livret-guide de l'excursion commune du Groupe Français d'Etude du Néogène et du Groupe Français de
239 Géomorphologie, 6 au 8 septembre 1996, 111 p.

240

241 Csato, I., Granjeon, D., Catuneanu, O. and Baum, G.R., 2012. A three dimensional stratigraphic model for the Messinian crisis
242 in the Pannonian Basin, eastern Hungary. *Basin Research*, **0**, 1-28.

243

244 Duvail, C., Gorini, C., Lofi, J., Strat, P.L., Clauzon, G. and Reis, A.D., 2005. Corrélation between onshore and offshore
245 pliocene-quadernary system tracts below the roussillon basin (Eastern Pyrenees, France). *Mar. Petrol. Geol.*, **22**, 747–756.

246

247 Duvail, C., 2008. Expression des facteurs régionaux et locaux dans l'enregistrement sédimentaire d'une marge passive.
248 exemple de la marge du golfe du lion, étudiée selon un continuum terre-mer. PhD thesis, University of Montpellier II.

249

250 Euzen, T., Joseph, P., Du Fornel, E., Lesur, S., Granjeon, D. and Guillocheau, F., 2004. Three-dimensional stratigraphic
251 modelling of the Grès d'Annot system, Eocene-Oligocene, SE-France. In: Deep-water sedimentation in the Alpine Foreland
252 Basin of SE France: New perspectives on the Grès d'Annot and related systems (P. Joseph, S. Lomas eds). *Geological Society*
253 *Special Publications*, **221**, 161-180.

254

255 Fairbanks, R., 1989. A 17,000-year glacio-eustatic sea level record: influence of glacial melting rates on the younger dryas
256 event and deep-ocean circulation. *Nature*, **342**, 637–641.

257

- 258 Fairbanks, R.G. and Matthews, R.K., 1978. The oxygen isotope stratigraphy of the Plesitocene reef tracts of Barbados, West
259 Indies. *Quaternary Research*, **10** (1), 181-196.
- 260
- 261 Genesseeux, M., Rehault, J. and Thomas, B., 1989. La marge continentale de la corse, *Bulletin de la Société Géologique de*
262 *France*, **5**, 339– 351.
- 263
- 264 Gorini, C., 1993. Géodynamique d'une marge passive: le golfe du lion (méditerranée occidentale). PhD thesis, University of
265 Paul Sabatier, Toulouse, 256 p.
- 266
- 267 Gorini, C., Mauffret, A., Guennoc, P. and Marrec, A. L., 1994. Structure of the gulf of lions (northwest mediterranean sea): A
268 review. In: Hydrocarbon and petroleum geology of France, A. Mascle (Ed), *Special Publication of the European Association*
269 *of Petroleum Geology*, Springer-Verlag, Berlin, **4**, 223–243.
- 270
- 271 Granjeon, D., 1997. Modélisation stratigraphique déterministe: conception et applications d'un modèle diffusif 3d
272 Multilithologique. PhD thesis, University of Rennes 1.
- 273
- 274 Granjeon, D. and Joseph P., 1999. Concepts and applications of a 3-d multiple lithology, diffusive model in stratigraphic
275 modelling. In: Numerical Experiments in Stratigraphy: Recent Advances in Stratigraphic and Sedimentologic Computer
276 Simulation, *SEPM Spec. Pub.* **62**, Tulsa, 197–210.
- 277
- 278 Guennoc, P., Gorini, C. and Mauffret A., 2000. Histoire géologique du golfe du lion et cartographie du rift oligo-aquitainien et
279 de la surface d'érosion messinienne. *Géologie de la France*, **3**, 67–97.
- 280
- 281 Haq, B., Hardenbol, J. and Vail P., 1987. Chronology of fluctuating sea levels since the triassic (250 million years ago to
282 present), *Science*, **235**, 1156–1166.
- 283
- 284 Head, M. and Gibbard, P., 2005. Early-middle pleistocene transitions : the land-ocean evidence. *Geological Society, London,*
285 *Spec. Pub.*, **247**.
- 286
- 287 Hodell, D., Benson, R., Kennett, J. and El Bied, K. R., 1989. Stable isotope stratigraphy of latest miocene sequences in
288 northwest morocco: the Bou Regreg section. *Paleoceanography*, **4**(4), 467–482.
- 289
- 290 Hsü, K., Cita, M. and Ryan, W., 1973. The origine of the Mediterranean evaporites. In: *Initial Report of the Deep Sea Drilling*

- 291 *Project 13*, W.B.F. Ryan, K.J. Hsü and al. (Eds), U.S. Government Printing Office, Washington, 1203–1231.
- 292
- 293 Jost, A., Fauquette, S., Kageyama, M., Krinner, G., Ramstein, G., Sue, J.P. and Violette, S., 2009. High resolution climate and
294 vegetation simulations of the Late Pliocene, a model-data comparison over western Europe and the Mediterranean region
295 *Climate of the past*, **5**(4), 585-606.
- 296
- 297 Jouet, G., 2007. Enregistrements stratigraphiques des cycles climatiques et glacio-eustatiques du quaternaire terminal. PhD
298 thesis, University of Bretagne Occidentale. <http://www.ifremer.fr/docelec>
- 299
- 300 Krijgsman, W., Hilgen, F., Raffi, I., Sierro, F. and Wilson, D., 1999b. Chronology, causes and progression of the messinian
301 salinity crisis. *Nature*, **400**(12), 652–655.
- 302
- 303 Lear, C., Elderfield H. and Wilson P., 2000. Cenozoic deep-sea temperatures from mg/ca in benthic foraminiferal calcite.
304 *Science*, **287**, 269–272.
- 305
- 306 LeDouaran, S., Burrus, J. and Avedik, F., 1984. Deep structure of the north-west mediterranean basin: results of two-ship
307 seismic survey. *Mar. Geol.*, **55**, 325–345.
- 308
- 309 Leroux, E., 2008. Simulations stratigraphiques des dépôts plio-quaternaires de la plate-forme du golfe du lion, Mémoire de
310 stade de Master2, Géosciences Marines de l'Université de Bretagne Occidentale.
- 311
- 312 Leroux, E., 2012. Quantification des flux sédimentaires et de la subsidence du bassin Provençal, PhD thesis, University of
313 Bretagne Occidentale, Brest, 455p., <http://www.ifremer.fr/docelec> or <http://www.archives-ouvertes.fr>
- 314
- 315 Lisiecki, L. and Raymo, M., 2005. A pliocene-pleistocene stack of 57 globally distributed benthic $\delta^{18}\text{O}$ records.
316 *Paleoceanography*, **20**, PA1003, doi:10-1029/2004PA001071.
- 317
- 318 Lofi, J., 2002. La crise de salinité messinienne : conséquences directes et différées sur l'évolution sédimentaire de la marge du
319 golfe du lion, PhD thesis, University of Sciences et Technics of Lille I, Lille, 261 p.
- 320
- 321 Lofi, J., Rabineau, M., Gorini, C., Berné, S., Clauzon, G., Clarens, P.D., Reis, A.D., Mountain, G.S., Ryan, W., Steckler, M.
322 and Fouchet, C., 2003. Plio-quaternary prograding clinof orm wedges of the Western Gulf of Lion continental margin (NW
323 Mediterranean) after the messinian salinity crisis. *Mar. Geol.* **198**, 289–317.

324

325 Malinverno, A. and Ryan, W., 1986. Extension in tyrrhenian sea and shortening in the apennines as result of arc migration
326 driven by sinking of the lithosphere. *Tectonophysics*, **5**, 227–254.

327

328 Mauffret, A., Pascal, G., Maillard, A. and Gorini, C., 1995. Tectonics and deep structure of the North-Western Mediterranean
329 basin. *Mar. Pet. Geol.*, **12**(6), 645–646.

330

331 Montigny, R., Edel, J. and Thuizat, R., 1981. Oligo-miocene rotation of sardinia: K-ar ages and paleomagnetism data of
332 tertiary volcanics. *Earth Planet. Sci. Lett.*, **54**, 261–271.

333

334 Olivet, J.-L., 1987. L'origine du bassin nord-occidental de la méditerranée du point de vue de la cinématique des plaques. In :
335 Profils ECORS. Golfe du Lion: Rapport d'implantation, J. Burrus and J-L. Olivet (Eds), IFP, Paris, 35 941-1, 10–49.

336

337 Olivet, J.-L., 1996. La cinématique de la plaque ibérique. *Bulletin du Centre de Recherche et d'Exploration, Production Elf*
338 *Aquitaine*, **20**, 131–195.

339

340 Popescu, S., Biltekin, D., Winter, H., Suc, J-P., Melinte-Dobrinescu, MC, Rabineau M. and Clauzon, G., 2010. Pliocene and
341 Early–Middle Pleistocene vegetation and climate changes at the European scale: long pollen records and climatostratigraphy.
342 *Quaternary International*, **219**(1-2), 152-167.

343

344 Rabineau, M., 2001. Un modèle géométrique et stratigraphique des séquences de dépôts quaternaires de la plate-forme du golfe
345 du lion: enregistrement des cycles glacioeustatiques de 100 000ans. PhD thesis, University of Rennes 1/ IFREMER.
346 <http://www.ifremer.fr/docelec>

347

348 Rabineau, M., Berné, S., Aslanian, D., Olivet, J.-L., Joseph, P., Guillocheau, F., Bourrillet, J.-L., Ledrezen, E. and Granjeon,
349 D., 2005. Sedimentary sequences in the Gulf of Lions: a record of 100,000 years climatic cycles. *Mar. Pet. Geol.*, **22**, 775–804.

350

351 Réhault, J.-P., Boillot, G. and Mauffret, A., 1984. The western mediterranean basin, geological evolution. *Mar. Geol.*, **55**, 447–
352 477.

353

354 Rio, D., Sprovieri, R., Thunell, R., Grazzini, C.V. and Glacon, G., 1990. Pliocene-Pleistocene paleoenvironmental history of
355 the Western Mediterranean: a synthesis of ODP site 653 results. In: *Proceedings of the Ocean Drilling Program, Scientific*
356 *Results*, K.A. Kastens, J. Mascle *et al.* (Eds), **107**.

357

358 Ryan, W., 1973. Geodynamic implications of the messinian crisis of salinity. In: C.W. Drooger (Ed.), Messinian Events in
359 Mediterranean, North-Holland Publ. Co., Amsterdam, Netherland, 26–38.

360

361 Savoye, B. and Piper, D., 1991. The messinian event on the margin of the mediterranean sea in the nice area, southern France.

362 *Mar. Geol.*, **97** (3-4), 279–304.

363

364 Shackleton, N., 1987. Oxygen isotopes, ice volume and sea level. *Quaternary Science Reviews*, **6** (3-4), 183–190.

365

366 Shackleton, N., Hall, M. and Pate, D., 1995. Pliocene stable isotope stratigraphy of site 846. *Proceedings of the Ocean Drilling*
367 *Program, Scientific Results*, **138**, 337–355.

368

369 Somme, T.O., Helland-Hansen, W., Granjeon, D., 2009. Impact of eustatic amplitude variations on shelf morphology,
370 sediment dispersal, and sequence stratigraphic interpretation: Icehouse versus greenhouse systems. *Geology*, **37**(7), 587-590.

371

372 Suc, J.P., Bertini, A, Combourrieu-Nebout, N., Diniz, F., Leroy, S., Russo-Ermolli, E., Zheng, Z., Bessais, E. and Ferrier, J.,
373 1995. Structure of west mediterranean vegetation and climate since 5.3My. *Acta Zool. Cracoviensia*, **38**, 3–16.

374

375 Waelbroeck, C., Labeyrie, L., Michel, E., Duplessy, J., McManus, J., Lambeck, K., Balbon, E. and Labracherie M., 2002. Sea-
376 level and deep water temperature changes derived from benthic foraminifera isotopic records. *Quaternary Science Reviews*, **21**
377 (1-3), 295–305.

378

379 Zachos, J., Pagani, M., Sloan, L., Thomas, E. and Billups, K., 2001. Trends, rythms and aberrations in global climate 65 My to
380 present. *Science*, **292**, 686–693.

381

382

383

384

385

386

387

388

389

390

391

392

393 **FIGURE CAPTIONS**

394

395 **Figure 1.** Location of the study area and dataset on the bathymetric map of the Gulf of Lions. Red line: LRM18 seismic profile
396 used in this study; black triangles: petroleum wells.

397

398 **Figure 2.** Interpreted LRM18 seismic reflection profile. The offlap-breaks are located with white dots; the first Pliocene
399 prism (p1) is also highlighted (yellow). Inset: the overall geometry of Pliocene-Quaternary strata shows prograding clinoforms
400 (or prisms) with a clear geometrical change of the Late Pliocene to Quaternary clinoforms (after yellow horizon p1), from
401 essentially prograding (dark green) to prograding-aggrading (light green).

402

403 **Figure 3.** Synthesis of LRM18 seismic interpretations on the shelf of the Gulf of Lions by different authors. Interpretation
404 from Rabineau (2001) in blue; interpretation from Lofi (2002) and Lofi et al. (2003) in green; interpretation from Duvail et al.
405 (2005) and Duvail (2008) in red. The interpreted chronostratigraphic markers have been digitalized, time-depth converted and
406 superimposed on the same vertical section with respective age estimates.

407

408 **Figure 4.** Simulations testing subsidence rates with a 100 000 years time-step (modified from Leroux, 2008).

409 Comparaison of LRM18 seismic profile interpretations (grey lines) with simulated geometries and deposits bathymetry
410 predicted by Dionisos (thick coloured lines). The simulations are run with a third order sea-level curve (Haq et al., 1988). A)
411 Simulation with a constant subsidence rate of 250 m/My at 70 km from the coast, then B1), B2), B3) using increasing
412 subsidence rates. Note that the change to overall prograding-aggrading pattern occurs without any change in the subsidence
413 rate. Note that we could not reconstitute the observations in B2 nor B3 when the increase of subsidence is too strong or with no
414 subsidence between 5.3 Ma and 2.6 Ma. Note also that in both cases, the observed height for the Early Pliocene clinoforms
415 could not be reproduced. Once the horizontal positions of the *offlap-breaks* along seismic profile have been adjusted, their
416 simulated depths are too deep (see the highlighted yellow area on the right). In such a subsidence scenario, the accommodation
417 which is created after 2.6 Ma increases too much the *topsets* slopes of the clinoforms already deposited. Note on the fictive
418 wells that sand is deposited at the shelf-break, whereas finer sediments (silt and shale) are deposited on the shelf and on the
419 slope (with a downstream decreasing granulometry).

420

421 **Figure 5** – Simulations testing sea-level curves

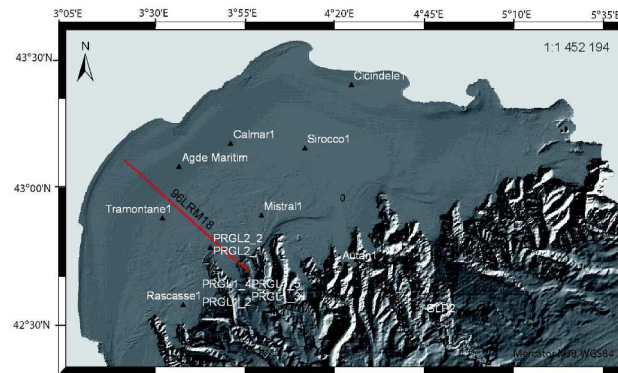
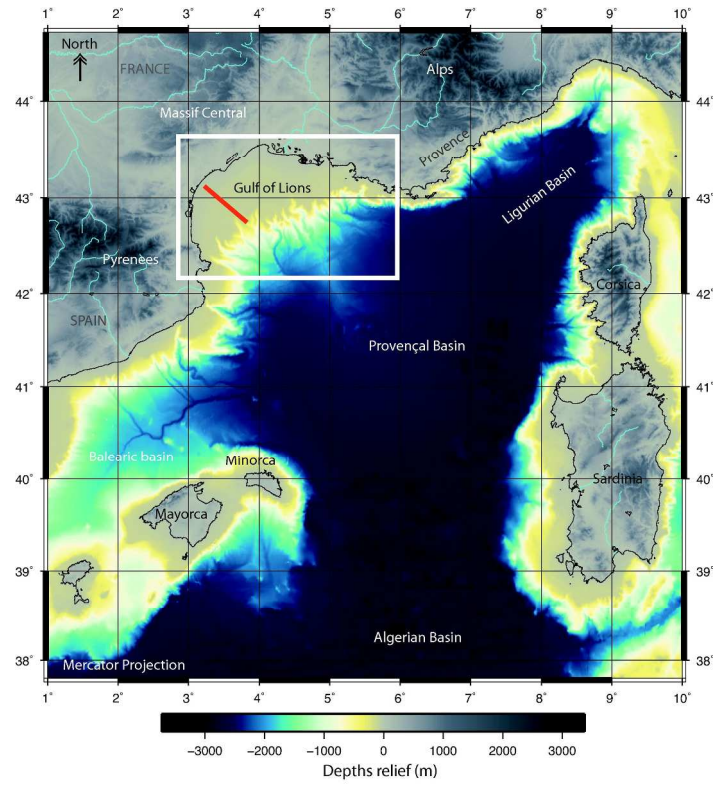
422 Comparison of simulated geometries (modified from Leroux, 2008) using (A) Haq et al. (1987) sea-level curve and (B) a
423 higher resolution sea-level curve resulting from $\delta^{18}\text{O}$ data (Lisiecki and Raymo, 2005).
424 Simulations are running with a 10 000 y time-step. All the others input parameters are identical in the both simulations (with
425 constant 45 km³/My sedimentary flux and 250 m/My subsidence rate on the time interval). The chronomarkers correspond to
426 the major sea-level falls (red) or to the Maximum Flooding Surface/MFS (blue). Black circles show offlap-break positions.

427

428 **Figure 6.** Evolution of the required sediment fluxes in our modellings in the case of a constant Plio-Quaternary subsidence
429 rate. These fluxes result from 10 000 years time step simulations with (A) third order eustatic curve (Haq et al., 1988) and (B)
430 (Lisiecki and Raymo, 2005) higher resolution eustatic curve.

431

432



Leroux et al., Figure 1

Figure 1. Location of the study area and dataset on the bathymetric map of the Gulf of Lions. Red line: LRM18 seismic profile used in this study; black triangles: petroleum wells.
204x342mm (300 x 300 DPI)

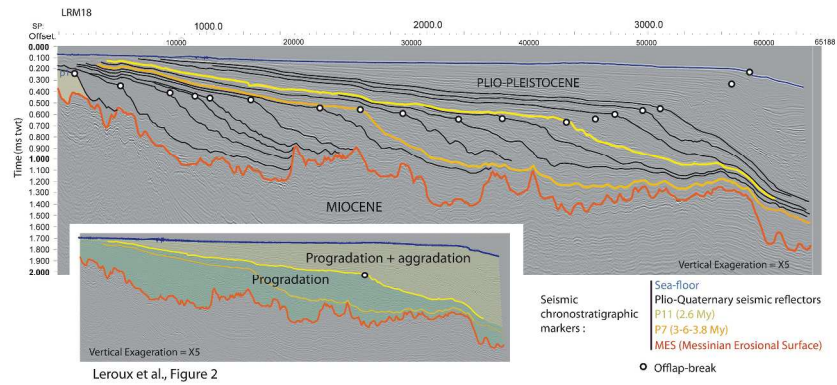


Figure 2. Interpreted LRM18 seismic reflection profile. The offlap-breaks are located with white dots; the first Pliocene prism (p1) is also highlighted (yellow). Inset: the overall geometry of Pliocene-Quaternary strata shows prograding clinofolds (or prisms) with a clear geometrical change of the Late Pliocene to Quaternary clinofolds (after yellow horizon p11), from essentially prograding (dark green) to prograding-aggrading (light green).

297x420mm (300 x 300 DPI)

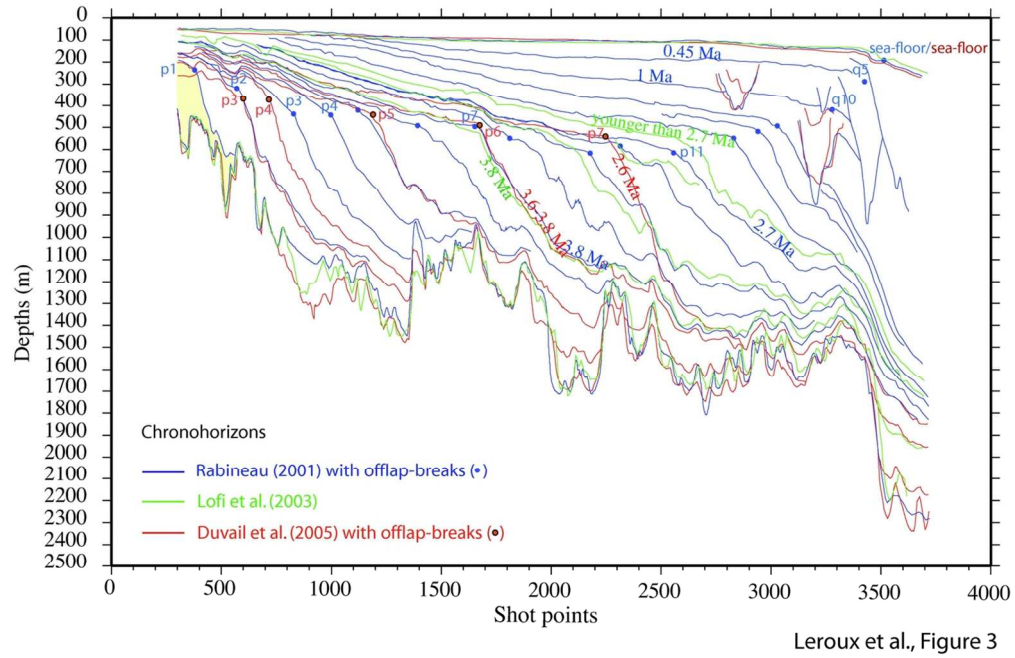
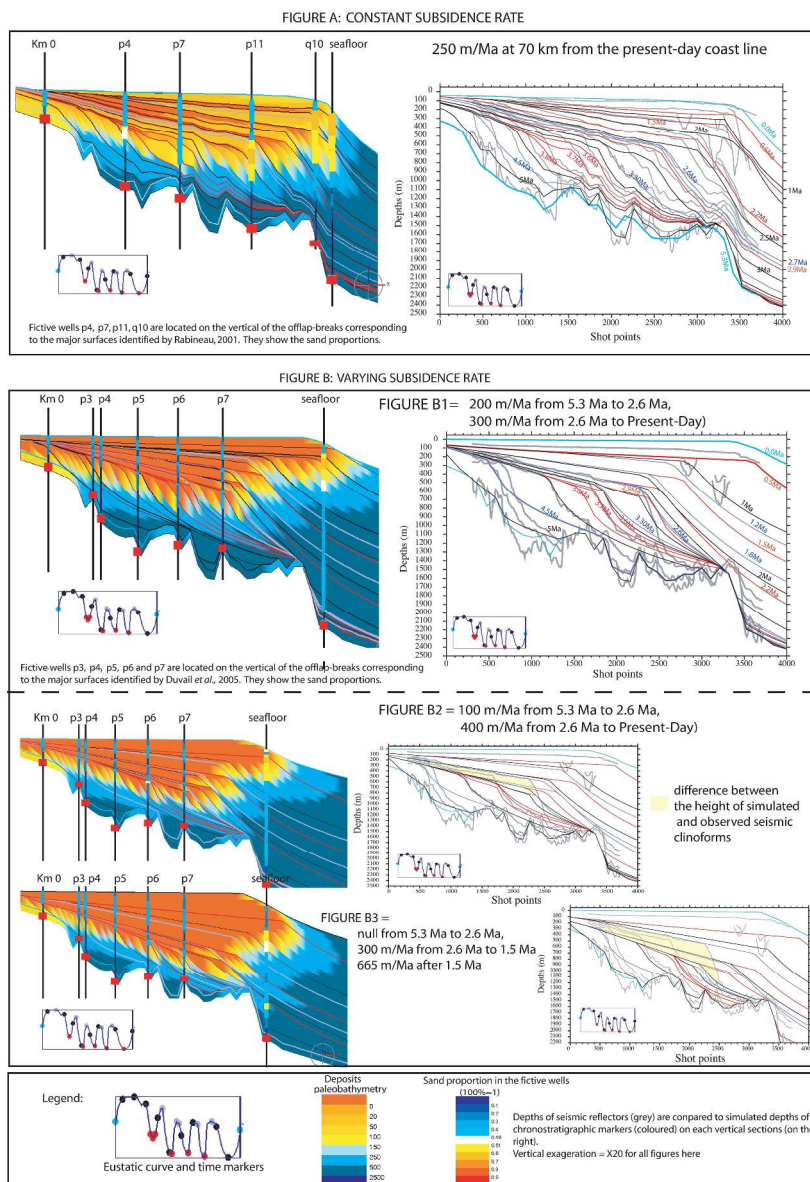


Figure 3. Synthesis of LRM18 seismic interpretations on the shelf of the Gulf of Lions by different authors. Interpretation from Rabineau (2001) in blue; interpretation from Lofi (2002) and Lofi et al. (2003) in green; interpretation from Duvail et al. (2005) and Duvail (2008) in red. The interpreted chronostratigraphic markers have been digitalized, time-depth converted and superimposed on the same vertical section with respective age estimates.
118x77mm (300 x 300 DPI)



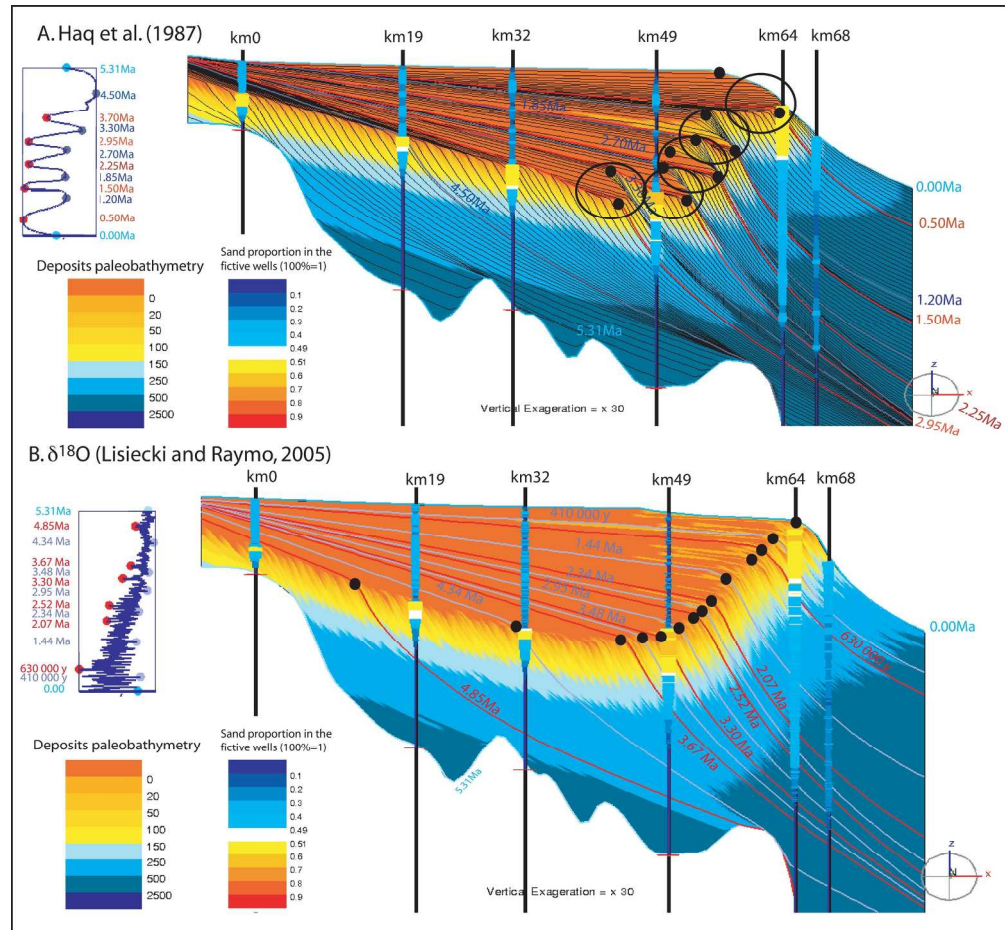
Leroux et al., Figure 4

Figure 4. Simulations testing subsidence rates with a 100 000 years time-step (modified from Leroux, 2008).

Comparison of LRM18 seismic profile interpretations (grey lines) with simulated geometries and deposits bathymetry predicted by Dionisos (thick coloured lines). The simulations are run with a third order sea-level curve (Haq et al., 1988). A) Simulation with a constant subsidence rate of 250 m/My at 70 km from the coast, then B1), B2), B3) using increasing subsidence rates. Note that the change to overall prograding-aggrading pattern occurs without any change in the subsidence rate. Note that we could not reconstitute the observations in B2 nor B3 when the increase of subsidence is too strong or with no subsidence between 5.3 Ma and 2.6 Ma. Note also that in both cases, the observed height for the Early Pliocene clinoforms could not be reproduced. Once the horizontal positions of the offlap-breaks along seismic profile have been adjusted, their simulated depths are too deep (see the highlighted yellow area on the right). In such a subsidence scenario, the accommodation which is created after 2.6 Ma increases too much the topsets slopes of the clinoforms already deposited. Note on the fictive wells that sand is deposited at the shelf-break, whereas

finer sediments (silt and shale) are deposited on the shelf and on the slope (with a downstream decreasing granulometry).

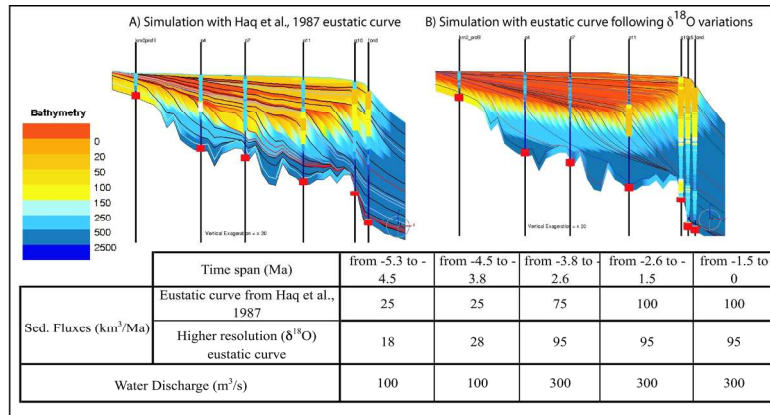
293x400mm (300 x 300 DPI)



Leroux et al., Figure 5

Figure 5 – Simulations testing sea-level curves
 Comparison of simulated geometries (modified from Leroux, 2008) using (A) Haq et al. (1987) sea-level curve and (B) a higher resolution sea-level curve resulting from $\delta^{18}\text{O}$ data (Lisiecki and Raymo, 2005). Simulations are running with a 10 000 y time-step. All the other input parameters are identical in the both simulations (with constant 45 km³/My sedimentary flux and 250 m/My subsidence rate on the time interval). The chronomarkers correspond to the major sea-level falls (red) or to the Maximum Flooding Surface/MFS (blue). Black circles show offlap-break positions.

200x190mm (300 x 300 DPI)



Leroux et al., Figure 6

Figure 6. Evolution of the required sediment fluxes in our modellings in the case of a constant Plio-Quaternary subsidence rate. These fluxes result from 10 000 years time step simulations with (A) third order eustatic curve (Haq et al., 1988) and (B) (Lisiecki and Raymo, 2005) higher resolution eustatic curve. 195x146mm (300 x 300 DPI)